Bioimaging of Hyaluronate–Interferon α Conjugates Using a Non-Interfering Zwitterionic Fluorophore

Ki Su Kim[†], **Hoon Hyun**[§,∥], **Jeong-A Yang**[‡], **Min Young Lee**[‡], **Hyemin Kim**[‡], **Seok-Hyun Yun**[†], **Hak Soo Choi**[§,*], and **Sei Kwang Hahn**[*,†,‡]

[†]Wellman Center for Photomedicine, Massachusetts General Hospital and Harvard Medical School, 65 Landsdowne Street, Cambridge, Massachusetts 02139, United States

[‡]Department of Materials Science and Engineering, Pohang University of Science and Technology (POSTECH), 77 Cheongam-ro, Nam-gu, Pohang, Kyungbuk 790-784, Korea

[§]Division of Hematology/Oncology, Department of Medicine, Beth Israel Deaconess Medical Center and Harvard Medical School, 330 Brookline Avenue, Boston, Massachusetts 02215, United States

[∥]Department of Biomedical Science, Chonnam National University Medical School, 160 Baekseo-ro, Dong-gu, Gwangju 501-746, Korea

Abstract

We conducted real-time bioimaging of the hyaluronate–interferon α (HA–IFNα) conjugate using a biologically inert zwitterionic fluorophore of ZW800-1 for the treatment of hepatitis C virus (HCV) infection. ZW800-1 was labeled on the IFNα molecule of the HA–IFNα conjugate to investigate its biodistribution and clearance without altering its physicochemical and targeting characteristics. Confocal microscopy clearly visualized the effective *in vitro* cellular uptake of the HA–IFNα conjugate to HepG2 cells. After verifying the biological activity in Daudi cells, we conducted the pharmacokinetic analysis of the HA–IFNα conjugate, which confirmed its target-specific delivery to the liver with a prolonged residence time longer than that of PEGylated IFNα. *In vivo* and *ex vivo* bioimaging of the ZW800-1-labeled HA–IFNα conjugate directly showed real-time biodistribution and clearance of the conjugate that are consistent with the biological behaviors analyzed by an enzyme-linked immunosorbent assay. Furthermore, the elevated level of OAS1 mRNA in the liver confirmed *in vivo* antiviral activity of HA–IFNα conjugates. With the data taken together, we could confirm the feasibility of ZW800-1 as a biologically inert fluorophore and target-specific HA–IFNα conjugate for the treatment of HCV infection.

*Corresponding Authors: Telephone: +1 617 667 6024. Fax: +1 617 667 0214. hchoi@bidmc.harvard.edu; Telephone: +82 54 279 2159. Fax: +82 54 279 2399. skhanb@postech.ac.kr.

ZW800-1   IFNα-ZW800-1   HA-IFNα-ZW800-1
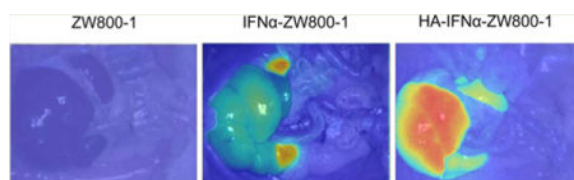
INTRODUCTION

Hepatitis C virus (HCV) is the main cause of chronic liver diseases,[1] infecting ~200 million people worldwide.[2] In addition, more than 350000 people die from liver diseases caused by HCV infection every year.[3] There have been numerous clinical trials[4,5] for the treatment of HCV infection, but the only outcome from the past is the clinical use of interferon α (IFNα) derivatives.[1,6] Currently, there are several kinds of polymer–IFNα conjugate formulations available for treating liver diseases. Among them, PEGylated interferon α (PEG–IFNα) has been successfully commercialized under the trade names PEGASYS and PEG-Intron.[7–9] However, PEGylation was intended to bypass liver for long-term circulation of biopharmaceuticals, which might not be a good strategy for the treatment of liver diseases. PEG–IFNα resulted in an unexpectedly low sustained virologic response of 39% in clinical tests.[10] Despite the recent announcement on two approved drugs and dozens more in the pipeline,[6] IFNα therapy remains an important remedy for the treatment of HCV infection.

Hyaluronate (HA), a biocompatible, biodegradable, and non-toxic polysaccharide, has been extensively investigated as a target-specific drug delivery carrier.[11,12] In our previous work, we successfully investigated the bioconjugation efficiency and *in vitro* and *in vivo* biological activity of the HA–IFNα conjugate for the treatment of HCV infection.[10] However, *in vivo* dynamics and clearance were not explored in detail without adequate imaging agents. The use of hydrophobic metal-containing quantum dots (QDots) as an imaging probe might result in alteration of the biological behaviors of the conjugates.[13–16] In addition, unconjugated or detached QDots might contaminate the target-specific HA in the body during excretion and metabolic processes, causing various side effects because of their inherent toxicity.[17,18] To circumvent these issues, a zwitterionic (ZW) fluorophore of ZW800-1 has been developed to investigate the *in vivo* mechanism, disease targeting, and biodistribution of biomolecules.[19,20] In addition, it can be easily conjugated to other biomolecules such as targeting moieties in the forms of an aptamer, a peptide, and a protein.

In this study, we conjugated a ZW-NIR fluorophore of ZW800-1 to the amine group of IFNα in HA–IFNα conjugates. Because ZW800-1 has a net charge of zero and an emission wavelength of 800 nm in the near-infrared (NIR) window, we could avoid potentially nonspecific tissue uptake and serum protein association,[19,20] allowing *in vivo* visualization for the long-term biodistribution and clearance of HA–IFNα conjugates without the first-pass effect of lipophilic bioconjugates.[21,22] After *in vitro, in vivo*, and *ex vivo* bioimaging of the ZW800-1-labeled HA–IFNα conjugate, we assessed the antiviral activity of HA–IFNα conjugates and discussed the feasibility of ZW800-1 as a biologically inert fluorophore for further bioimaging applications and target-specific HA–IFNα conjugates for the treatment of HCV infection.

EXPERIMENTAL SECTION

Synthesis of the HA–IFNa–ZW800-1 Conjugate

The HA–IFNa conjugate was synthesized as we previously reported.[30] PEG–IFNa (PEG-Intron, Merck) was used as a positive control. To synthesize ZW800-1 NHS ester, 2 equiv of dipyrrolidino(*N*-succinimidyloxy)carbenium hexafluorophosphate in dimethyl sulfoxide was mixed with 5 equiv of diisopropylethylamine at room temperature in the dark.[19,20] After being stirred for 3 h, the reaction mixture was precipitated with an excess of ethyl acetate. The precipitate was washed with a 1:1 mixture of ethyl acetate and acetone thrice and dried in vacuum. The purity was confirmed to be higher than 98% by reversed-phase high-performance liquid chromatography (770 nm absorbance) and matrix-assisted laser desorption ionization time of flight. The primary amine on IFNa in the HA–IFNa conjugate was conjugated with the ZW800-1 NHS ester at a 1:2 (IFNa:dye) ratio in PBS (pH 7.8), followed by purification using gel filtration chromatography (GFC). For comparison, the IFNa–ZW800-1 conjugate was also prepared by the conjugation of free IFNa with the same amount of ZW800-1 NHS ester.

In Vitro Bioimaging of the HA–IFNa–ZW800-1 Conjugate

Human hepatocarcinoma cells (HepG2, ATCC, Manassass, VA) were cultured at 37 °C and 5% CO_2 in DMEM containing 10% fetal bovine serum (FBS) and 10 IU/mL antibiotics (penicillin). HepG2 cells (5×10^4) were seeded and incubated in a six-well culture dish for 24 h, followed by the replacement of medium with DMEM containing 1% FBS. One milliliter of ZW800-1, IFNa–ZW800-1 conjugate, or HA–IFNa–ZW800-1 conjugate was added to each well at a concentration of 2 μM and incubated for 2 h.[15] Cells were washed with PBS, fixed with 4% paraformaldehyde in PBS, washed again with PBS twice, and observed with a fluorescence microscope at a magnification of 200×. The internalized HA–IFNa–ZW800-1 conjugate in the cytoplasm was excited at 700 nm and visualized through a long pass emission filter (Chroma Technology Co., Brattleboro, VT).

In Vitro Biological Activity of the HA–IFNa Conjugate

Human Daudi cells (Korean Cell Line Bank, Seoul, Korea) were cultured in RPMI 1640 (Mediatech, Herndon, VA) supplemented with 10% FBS and 1% antibiotics in a humidified incubator at 37 °C under 5% CO_2 in air. Cells were seeded onto sterilized 18 mm diameter glass coverslips in 96-well plates (2×10^4 cells per well). A serial dilution of protein samples was prepared in assay medium, and 50 μL of the diluted protein samples was added to the test wells in triplicate. The plates were incubated at 37 °C in a humidified 5% CO_2 tissue culture incubator for 4 days. Then, 20 μL of Cell Titer 96 AQueous One Solution Reagent (Promega, Madison, WI) was added to each well, which was incubated additionally at 37 °C for 2 h. The absorbance was measured at 490 nm using a microplate reader (EMax, Molecular Devices).

In Vivo and *ex Vivo* Bioimaging of the HA–IFNa–ZW800-1 Conjugate

Animals were housed in an AAALAC-certified facility. All animal studies were performed under the supervision of BIDMC IACUC in accordance with approved institutional protocol

058-2014. For intraoperative hepatic imaging, male Sprague-Dawley (SD) rats weighing 250–300 g were purchased from Charles River Laboratories (Wilmington, MA). Prior to surgery, animals were anesthetized with 100 mg/kg of ketamine and 10 mg/kg of xylazine intraperitoneally (Webster Veterinary, Fort Devens, MA). After intravenous injection of ZW800-1, the IFNα–ZW800-1 conjugate, or the HA–IFNα–ZW800-1 conjugate (50 nmol) at the same concentration of ZW800-1 into SD rats, intraoperative imaging was performed at each designated time point up to 24 h to observe the initial biodistribution and clearance. For long-term imaging, SD rats were sacrificed 1, 2, 4, 7, and 10 days after injection of HA–IFNα–ZW800-1 conjugates (50 nmol), and their organs were dissected for quantitative fluorescence imaging. *In vivo* and *ex vivo* images were obtained by merging the optical image and the corresponding fluorescence image.

Intraoperative Image Analysis

As we previously described in detail,[19] bioimaging was conducted using a FLARE imaging system. At predetermined time points, the fluorescence (FL) and background (BG) intensities of a region of interest (ROI) over each organ and/or tissue were quantified using custom FLARE software. The signal-to-background ratio (SBR) was calculated using ImageJ version 1.45q. All NIR fluorescence images were normalized identically for all conditions. At least three to five animals were analyzed at each time point.

Biodistribution of the HA–IFNα Conjugate by an Enzyme-Linked Immunosorbent Assay (ELISA)

After intravenous injection of PEG–IFNα and HA–IFNα conjugates containing 70 μg of IFNα into SD rats (250 g), animals were sacrificed 1, 3, 7, and 14 days postinjection. The blood serum was collected by centrifugation at 3500 rpm for 30 min, and the same weight of liver tissue was homogenized for 10 min, followed by sonication for 1 min. The IFNα content in the blood and liver tissue was quantified with IFNα ELISA kits (PBL InterferonSource, Piscataway, NJ).

In Vivo Antiviral Effect of HA–IFNα Conjugates

After subcutaneous injection of PEG–IFNα and HA–IFNα conjugates containing 70 μg of IFNα into SD rats (250 g), animals were sacrificed 2 and 4 days postinjection. The same weight of liver tissues was collected for the analysis of IFNα content by an ELISA and OAS1-expressing mRNA (OAS1 mRNA) level by reverse transcriptase polymerase chain reaction (RT-PCR) (Alpha Unit Block Assembly for PTC DNA Engine Systems, MJ Research).

Statistical Analysis

Statistical analysis was conducted via the two-way analysis of variance (ANOVA) test using SigmaPlot 10.0 (Systat Software Inc., San Jose, CA). A P value of <0.05 was considered statistically significant. Data are expressed as means ± the standard deviation from several separate experiments ($n = 3$).

RESULTS AND DISCUSSION

Synthesis of the HA–IFNa–ZW800-1 Conjugate

Figure 1a shows the schematic illustration for dual targeted delivery of HA–IFNa conjugates for the treatment of HCV infection. The HA–IFNa conjugates can interact with both the receptor and the HA receptor on liver sinusoidal endothelial cells (LSEC), penetrating into the perisinusoidal space (space of Disse) through LESC fenestration.[15,23,24] Accordingly, HA–IFNa conjugates can be efficiently delivered to and accumulate in the liver. As a proof of concept, we synthesized and compared HA–IFNa conjugates (MW of HA = 17 kDa) with PEG-Intron (PEG–IFNa), a commercially available PEGylated IFNa (MW of PEG = 12 kDa). The lysine residue of IFNa was directly conjugated with ZW800-1 NHS ester by the conventional NHS ester reaction (Figure 1b). The resulting HA–IFNa–ZW800-1 conjugate was purified by GFC to remove unconjugated fluorophores.

As shown in Figure 2, the GFC trace shows the successful conjugation with two isolated peaks indicating the HA–IFNa–ZW800-1 conjugate (2.5 min) and unreacted ZW800-1 (5.5 min). The purified HA–IFNa–ZW800-1 conjugate was characterized with a spectrophotometer ($\lambda_{max\ Abs}$ = 775 nm; $\lambda_{max\ FL}$ = 788 nm). The conjugation efficiency was estimated from the ratio of extinction coefficients of ZW800-1 (ε_{772} = 249000 M^{-1} cm^{-1}) and IFNa (ε_{280} = 18000 M^{-1} cm^{-1}) with correction for 5% measured absorbance at 280 nm due to ZW800-1. The calculated labeling ratios for the HA–IFNa–ZW800-1 and IFNa–ZW800-1 conjugates were 0.215 and 0.273, respectively, which were determined by using the formula (Abs$_{772}$/ε_{772})/[(Abs$_{280}$ − 0.05 × Abs$_{772}$)/ε_{280}]. We purposely conjugated small numbers of dyes on the protein to prevent the disruption of activity by the conjugated fluorophores. With the minimal conjugation of ZW800-1, it was possible to visualize the HA–IFNa conjugate because of its high quantum yield (QY = 15%) and high extinction coefficient (ε = 249000 M^{-1} cm^{-1}), as we reported elsewhere.[19,20]

In Vitro Biological Activity of the HA–IFNa Conjugate

Figure 3a shows fluorescence microscopic images for *in vitro* cellular uptake of ZW800-1, IFNa–ZW800-1, and HA–IFNa–ZW800-1 conjugates into human hepatocarcinoma HepG2 cells. The rate of intracellular uptake of HA–IFNa–ZW800-1 conjugates was significantly higher than that of IFNa–ZW800-1 (*$P < 0.05$) or ZW800-1 alone (***$P < 0.001$) as shown in Figure 3b. Because hepatocellular carcinoma HepG2 cells have both IFNa and HA receptors,[15,25,26] the HA–IFNa conjugate can easily bind to the cells by the dual targeting effect of HA and IFNa. In addition, zwitterionic ZW800-1 has no affinity for the cellular membrane[19,20] without interfering with the *in vitro* cellular uptake of the HA–IFNa–ZW800-1 conjugate via HA receptor-mediated endocytosis.[11–13]

Figure 3c shows the *in vitro* biological activity of the HA–IFNa conjugate, which was confirmed by an antiproliferation assay using human B-lymphoblasts of Daudi cells. Daudi cells are known to be arrested in the G_0/G_1 phase of the cell cycle in the presence of IFNa.[10,27] The antiproliferation activity of the HA–IFNa conjugate was compared with those of PEG–IFNa and IFNa by measuring the concentration for 50% inhibition of cell growth (IC$_{50}$). The antiproliferation effect of the HA–IFNa (IC$_{50}$ = 165.8 pg/mL) conjugate

was significantly lower than that of native IFNα (IC$_{50}$ = 6.6 pg/mL; **P < 0.01) but comparable to that of PEG–IFNα (IC$_{50}$ = 70.0 pg/mL; P > 0.05). Because HA is biodegradable in the body, the biological activity of the HA–IFNα conjugate might increase after degradation by hyaluronidase in the body.

Pharmacokinetics of the HA–IFNα Conjugate

Because the residence time of IFNα in blood is significantly important for therapeutic efficacy,[28,29] we analyzed the amount of PEG–IFNα and HA–IFNα conjugates in the blood serum and the liver (Figure 4). After the injection of PEG–IFNα and HA–IFNα conjugates containing 70 μg of IFNα intravenously into SD rats, blood serum was collected at predetermined time points, and the liver was dissected and homogenized to measure the IFNα content by an ELISA. While PEG–IFNα was predominantly detected in the bloodstream on day 1 (***P < 0.001) and day 3 (**P < 0.01), HA–IFNα conjugates mainly accumulated in the liver on days 1 and 3 (**P < 0.01), remaining for up to 14 days postinjection. The results clearly indicate that the HA–IFNα conjugate can be target-specifically delivered to the liver in comparison to PEG–IFNα. Remarkably, the HA–IFNα conjugate remained longer in the liver than PEG–IFNα with a significant difference on days 7 and 14. The presence of PEG–IFNα was minimal and similar to that of the negative control in 7 days (P > 0.05). As well-known, PEGylation is intended to increase the blood circulation of conjugated therapeutics bypassing the liver. However, nonspecifically delivered PEG–IFNα was reported to cause serious side effects after repeated injections.[30] On the contrary, there are abundant HA receptors in the liver, including CD44 and HARE, which can promote the active uptake of HA–IFNα conjugates to the liver synergistically and concurrently with the existing IFNα receptors.[11] Armed with these results, we further investigated the long-term biodistribution and clearance of HA–IFNα–ZW800-1 conjugates *in vivo*.

Real-Time Biodistribution of the HA–IFNα–ZW800-1 Conjugate

As shown in Figure 5, NIR fluorescence imaging with the FLARE system visualized the real-time intraoperative biodistribution of HA–IFNα–ZW800-1 conjugates after injection of 50 nmol of the conjugate via the penile vein into SD rats (Supporting Video 1). As controls, ZW800-1 and the IFNα–ZW800-1 conjugate were also tested for compar-ison.[17,18] ZW800-1 was distributed into the whole body in 30 min and cleared out within 4 h through kidneys to bladder without nonspecific uptake in major organs.[19,20] Almost no fluorescence signal remained in the liver, and >75% of the injected dose was found in the bladder. On the other hand, both IFNα–ZW800-1 and HA–IFNα–ZW800-1 conjugates saturated kidneys first and then gradually accumulated in the liver between 30 and 240 min. The intensity of IFNα–ZW800-1 signals was maximal in the liver at 4 h, whereas the HA–IFNα–ZW800-1 conjugate steadily accumulated in the liver for up to 24 h.

Figure 6 shows the anatomic analysis of dissected organs 24 h post-intravenous injection of ZW800-1, IFNα–ZW800-1, and HA–IFNα–ZW800-1 conjugate. The level of targeted delivery of the HA–IFNα–ZW800-1 conjugate to the liver was significantly higher than those of two controls (***P < 0.001). Although the biodistribution trend of IFNα–ZW800-1 was similar to that of the HA–IFNα–ZW800-1 conjugate, the longitudinal uptake was

different in the liver and kidney. In accordance with the results in Figure 5, IFNa–ZW800-1 was rapidly degraded and accumulated in the kidney, showing the highest level in 24 h. However, the HA–IFNa–ZW800-1 conjugate gradually decreased in the kidney and increased in the liver with increasing time. Because HA receptors of CD44 and LYVE-1 are highly expressed on renal parenchymal cells[31] and in the renal lymphatic vessel,[32] HA–IFNa–ZW800-1 conjugates showed a high rate of uptake in the kidney. In addition, a high rate of uptake of the HA–IFNa–ZW800-1 conjugate in the spleen also resulted from the high level of expression of HA receptors on lymphatics.[32] The SBR of the HA–IFNa–ZW800-1 conjugate in the liver was remarkably higher for up to 24 h postinjection. The results clearly indicate that HA–IFNα–ZW800-1 conjugates can be target-specifically delivered to the liver.

Long-Term Biodistribution of the HA–IFNa–ZW800-1 Conjugate

Because the HA–IFNa–ZW800-1 conjugate showed the highest rate of uptake to the liver 24 h postinjection, we further investigated the long-term clearance of the conjugate in the body (Figure 7). SD rats were injected intravenously with 50 nmol of the HA–IFNa–ZW800-1 conjugate and sacrificed every 24 h up to 10 days. The fluorescence intensity in the liver was the highest at day 1 postinjection and gradually decreased over the course of 10 days. The results were well matched with our previous data as reported else-where.[11] All the remaining tissues and organs except liver, kidney, and spleen showed very minimal uptake, reflecting the possibility of the HA–IFNa–ZW800-1 conjugate for target-specific treatment of liver diseases without potential side effects by nonspecific uptake. Despite wide applications of IFNa and PEG–IFNa for the treatment of HCV infection, the repeated injection was known to cause significant side effects, including renal dysfunction and capillary leak syndrome.[33,34]

In Vivo Antiviral Effect of HA–IFNa Conjugates

As a feasibility study for clinical applications, HA–IFNa conjugates were subcutaneously injected into SD rats for the analysis of IFNα content by an ELISA and OAS1 mRNA levels by realtime PCR in the liver tissues 2 and 4 days postinjection (Figure 8). After injection of the HA–IFNa conjugate, the amount of IFNa was 3.3- and 1.8-fold higher in the liver than those of the control and PEG–IFNa in 2 days, respectively, reflecting the target-specific delivery of HA–IFNa conjugates to the liver (Figure 8a). In contrast, PEG–IFNa was not detected so much in the liver compared to HA–IFNa conjugates. As is well-known, PEGylation is intended to bypass the liver for long-term circulation of IFNa in the body. The results indirectly indicate that HA–IFNa conjugates can be more effective than PEG–IFNa for the treatment of HCV infection.

After that, the antiviral activity of HA–IFNa conjugates was investigated by measuring the level of OAS1 mRNA in the liver using RT-PCR. The antiviral activity of IFNa is highly related to the expression of OAS1, which is the essential protein for innate immune responses to viral infection.[30,35,36] Figure 8b shows the relative expression levels of the OAS1 gene by RT-PCR after subcutaneous injection of the control, PEG-IFNa, and HA–IFNa conjugate. In accordance with the biodistribution data, the OAS1 mRNA level increased more significantly after subcutaneous injection of the HA–IFNa conjugate than

the control and PEG–IFNa. The results were well matched with our previous data after intravenous injection of the HA–IFNa conjugate.[30] The elevated level of OAS1 mRNA was maintained for >4 days (Figure 8b). With the data taken together, we could confirm the feasibility of the HA–IFNa conjugate for the treatment of HCV infection and possibly hepatocellular carcinoma.[25,26]

CONCLUSION

We have successfully investigated the intrinsic biodistribution and clearance of the HA–IFNa conjugate for the treatment of HCV infection using a zwitterionic and nonsticky NIR fluorophore of ZW800-1. The short-term and long-term delivery and accumulation of the HA–IFNa conjugate in the liver were significant because of the synergistic effect of HA and IFNa receptors in the liver. The long-term *in vivo* and *ex vivo* bioimaging was also helpful for understanding the fate of bioconjugates, i.e., biodistribution and clearance in each tissue. Furthermore, we could confirm the antiviral activity of HA–IFNa conjugates from the elevated level of OAS1 mRNA in the liver by the analysis of RT-PCR. All these results lay the foundation for investigating the pharmacoki-netics and efficacy of the HA–IFNa conjugate as a new therapeutic drug for the treatment of HCV infection and possibly hepatocellular carcinoma.

Supplementary Material

Refer to Web version on PubMed Central for supplementary material.

Acknowledgments

References

1. Tan S-L, Pause A, Shi Y, Sonenberg N. Hepatitis C therapeutics: current status and emerging strategies. Nat Rev Drug Discovery. 2002; 1:867–881. [PubMed: 12415247]

2. Gravitz L. Introduction: A smouldering public-health crisis. Nature. 2011; 474:S2–S4. [PubMed: 21666731]

3. Perz JF, Armstrong GL, Farrington LA, Hutin YJF, Bell BP. The contributions of hepatitis B virus and hepatitis C virus infections to cirrhosis and primary liver cancer worldwide. J Hepatol. 2006; 45:529–538. [PubMed: 16879891]

4. Fellay J, Thompson AJ, Ge D, Gumbs CE, Urban TJ, Shianna KV, Little LD, Qiu P, Bertelsen AH, Watson M, Warner A, Muir AJ, Brass C, Albrecht J, Sulkowski M, McHutchison JG, Goldstein DB. ITPA gene variants protect against anaemia in patients treated for chronic hepatitis C. Nature. 2010; 464:405–408. [PubMed: 20173735]

5. Thomas DL, Thio CL, Martin MP, Qi Y, Ge D, O'hUigin C, Kidd J, Kidd K, Khakoo SI, Alexander G, Goedert JJ, Kirk GD, Donfield SM, Rosen HR, Tobler LH, Busch MP, McHutchison JG, Goldstein DB. Carrington MGenetic variation in IL28B and spontaneous clearance of hepatitis C virus. Nature. 2009; 461:798–801. [PubMed: 19759533]

6. Schlutter J. Therapeutics: New drugs hit the target. Nature. 2011; 474:S5–S7. [PubMed: 21666733]

7. Wang Y-S, Youngster S, Grace M, Bausch J, Bordens R, Wyss DF. Structural and biological characterization of pegylated recombinant interferon alpha-2b and its therapeutic implications. Adv Drug Delivery Rev. 2002; 54:547–570.

8. Bailon P, Palleroni A, Schaffer CA, Spence CL, Fung W-J, Porter JE, Ehrlich GK, Pan W, Xu Z-X, Modi MW, Farid A, Berthold W, Graves M. Rational Design of a Potent, Long-Lasting Form of Interferon: A 40 kDa Branched Polyethylene Glycol-Conjugated Interferon a-2a for the Treatment of Hepatitis C. Bioconjugate Chem. 2001; 12:195–202.

9. Foser S, Schacher A, Weyer KA, Brugger D, Dietel E, Marti S, Schreitmuller T. Isolation, structural characterization, and antiviral activity of positional isomers of monopegylated interferon alpha-2a (PEGASYS). Protein Expression Purif. 2003; 30:78–87.

10. Yang J-A, Park K, Jung H, Kim H, Hong SW, Yoon SK, Hahn SK. Target specific hyaluronic acid-interferon alpha conjugate for the treatment of hepatitis C virus infection. Biomaterials. 2011; 32:8722–8729. [PubMed: 21872329]

11. Oh EJ, Park K, Kim KS, Kim J, Yang J-A, Kong J-H, Lee MY, Hoffman AS, Hahn SK. Target specific and long-acting delivery of protein, peptide, and nucleotide therapeutics using hyaluronic acid derivatives. J Controlled Release. 2010; 141:2–12.

12. Stern R. Hyaluronan catabolism: a new metabolic pathway. Eur J Cell Biol. 2004; 83:317–325. [PubMed: 15503855]

13. Goh EJ, Kim KS, Kim YR, Jung HS, Beack S, Kong WH, Scarcelli G, Yun SH, Hahn SK. Bioimaging of Hyaluronic Acid Derivatives Using Nanosized Carbon Dots. Biomacromolecules. 2012; 13:2554–2561. [PubMed: 22804331]

14. Kim J, Kim KS, Jiang G, Kang H, Kim S, Kim B-S, Park MH, Hahn SK. In vivo real-time bioimaging of hyaluronic acid derivatives using quantum dots. Biopolymers. 2008; 89:1144–1153. [PubMed: 18690665]

15. Kim KS, Hur W, Park S-J, Hong SW, Choi JE, Goh EJ, Yoon SK, Hahn SK. Bioimaging for Targeted Delivery of Hyaluronic Acid Derivatives to the Livers in Cirrhotic Mice Using Quantum Dots. ACS Nano. 2010; 4:3005–3014. [PubMed: 20518553]

16. Kim KS, Kim S, Beack S, Yang J-A, Yun SH, Hahn SK. In vivo real-time confocal microscopy for target-specific delivery of hyaluronic acid-quantum dot conjugates. Nanomedicine. 2012; 8:1070–1073. [PubMed: 22687895]

17. Choi HS, Ipe BI, Misra P, Lee JH, Bawendi MG, Frangioni JV. Tissue- and Organ-Selective Biodistribution of NIR Fluorescent Quantum Dots. Nano Lett. 2009; 9:2354–2359. [PubMed: 19422261]

18. Soo Choi H, Liu W, Misra P, Tanaka E, Zimmer JP, Itty Ipe B, Bawendi MG, Frangioni JV. Renal clearance of quantum dots. Nat Biotechnol. 2007; 25:1165–1170. [PubMed: 17891134]

19. Choi HS, Gibbs SL, Lee JH, Kim SH, Ashitate Y, Liu F, Hyun H, Park G, Xie Y, Bae S, Henary M, Frangioni JV. Targeted zwitterionic near-infrared fluorophores for improved optical imaging. Nat Biotechnol. 2013; 31:148–153. [PubMed: 23292608]

20. Choi HS, Nasr K, Alyabyev S, Feith D, Lee JH, Kim SH, Ashitate Y, Hyun H, Patonay G, Strekowski L, Henary M, Frangioni JV. Synthesis and In Vivo Fate of Zwitterionic Near-Infrared Fluorophores. Angew Chem Int Ed. 2011; 50:6258–6263.

21. Tanaka E, Choi HS, Humblet V, Ohnishi S, Laurence RG, Frangioni JV. Real-time intraoperative assessment of the extrahepatic bile ducts in rats and pigs using invisible near-infrared fluorescent light. Surgery. 2008; 144:39–48. [PubMed: 18571583]

22. Ballou B, Fisher GW, Deng JS, Hakala TR, Srivastava M, Farkas DL. Cyanine fluorochrome-labeled antibodies in vivo: assessment of tumor imaging using Cy3, Cy5, Cy5.5, and Cy7. Cancer Detect Prev. 1998; 22:251–257. [PubMed: 9618048]

23. Warren A, Le Couteur DG, Fraser R, Bowen DG, McCaughan GW, Bertolino P. T lymphocytes interact with hepatocytes through fenestrations in murine liver sinusoidal endothelial cells. Hepatology. 2006; 44:1182–1190. [PubMed: 17058232]

24. Gaumet M, Vargas A, Gurny R, Delie F. Nanoparticles for drug delivery: The need for precision in reporting particle size parameters. Eur J Pharm Biopharm. 2008; 69:1–9. [PubMed: 17826969]

25. Damdinsuren B, Nagano H, Wada H, Noda T, Natsag J, Marubashi S, Miyamoto A, Takeda Y, Umeshita K, Doki Y, Dono K, Monden M. Interferon alpha receptors are important for

antiproliferative effect of interferon-α against human hepatocellular carcinoma cells. Hepatol Res. 2007; 37:77–83. [PubMed: 17300701]

26. Melén K, Keskinen P, Lehtonen A, Julkunen I. Interferon-induced gene expression and signaling in human hepatoma cell lines. J Hepatol. 2000; 33:764–772. [PubMed: 11097485]

27. Gisslinger H, Kurzrock R, Gisslinger B, Jiang S, Li S, Virgolini I, Woloszczuk W, Andreeff M, Talpaz M. Autocrine cell suicide in a Burkitt lymphoma cell line (Daudi) induced by interferon *a*: involvement of tumor necrosis factor as ligand for the CD95 receptor. Blood. 2001; 97:2791–2797. [PubMed: 11313273]

28. Bell SJ, Fam CM, Chlipala EA, Carlson SJ, Lee JI, Rosendahl MS, Doherty DH, Cox GN. Enhanced Circulating Half-Life and Antitumor Activity of a Site-Specific Pegylated Interferon-*a* Protein Therapeutic. Bioconjugate Chem. 2008; 19:299–305.

29. Glue P, Fang JWS, Rouzier-Panis R, Raffanel C, Sabo R, Gupta SK, Salfi M, Jacobs S. Pegylated interferon-[alpha]2b: Pharmacokinetics, pharmacodynamics, safety, and preliminary efficacy data[ast]. Clin Pharmacol Ther. 2000; 68:556–567. [PubMed: 11103758]

30. Yang JA, Park K, Jung H, Kim H, Hong SW, Yoon SK, Hahn SK. Target specific hyaluronic acid-interferon alpha conjugate for the treatment of hepatitis C virus infection. Biomaterials. 2011; 32:8722–9. [PubMed: 21872329]

31. Wüthrich RP. The proinflammatory role of hyaluronan–CD44 interactions in renal injury. Nephrol Dial Transpl. 1999; 14:2554–2556.

32. Oliver G. Lymphatic vasculature development. Nat Rev Immunol. 2004; 4:35–45. [PubMed: 14704766]

33. Dusheiko G. Side effects of α interferon in chronic hepatitis C. Hepatology. 1997; 26:112S–121S. [PubMed: 9305675]

34. Lechner J, Krall M, Netzer A, Radmayr C, Ryan MP, Pfaller W. Effects of interferon [agr]-2b on barrier function and junctional complexes of renal proximal tubular LLC-PK1 cells. Kidney Int. 1999; 55:2178–2191. [PubMed: 10354267]

35. Yuan L, Wang J, Shen W-C. Lipidization of human interferon-alpha: A new approach toward improving the delivery of protein drugs. J Controlled Release. 2008; 129:11–17.

36. Shrivastava S, Raychoudhuri A, Steele R, Ray R, Ray RB. Knockdown of autophagy enhances the innate immune response in hepatitis C virus-infected hepatocytes. Hepatology. 2011; 53:406–414. [PubMed: 21274862]

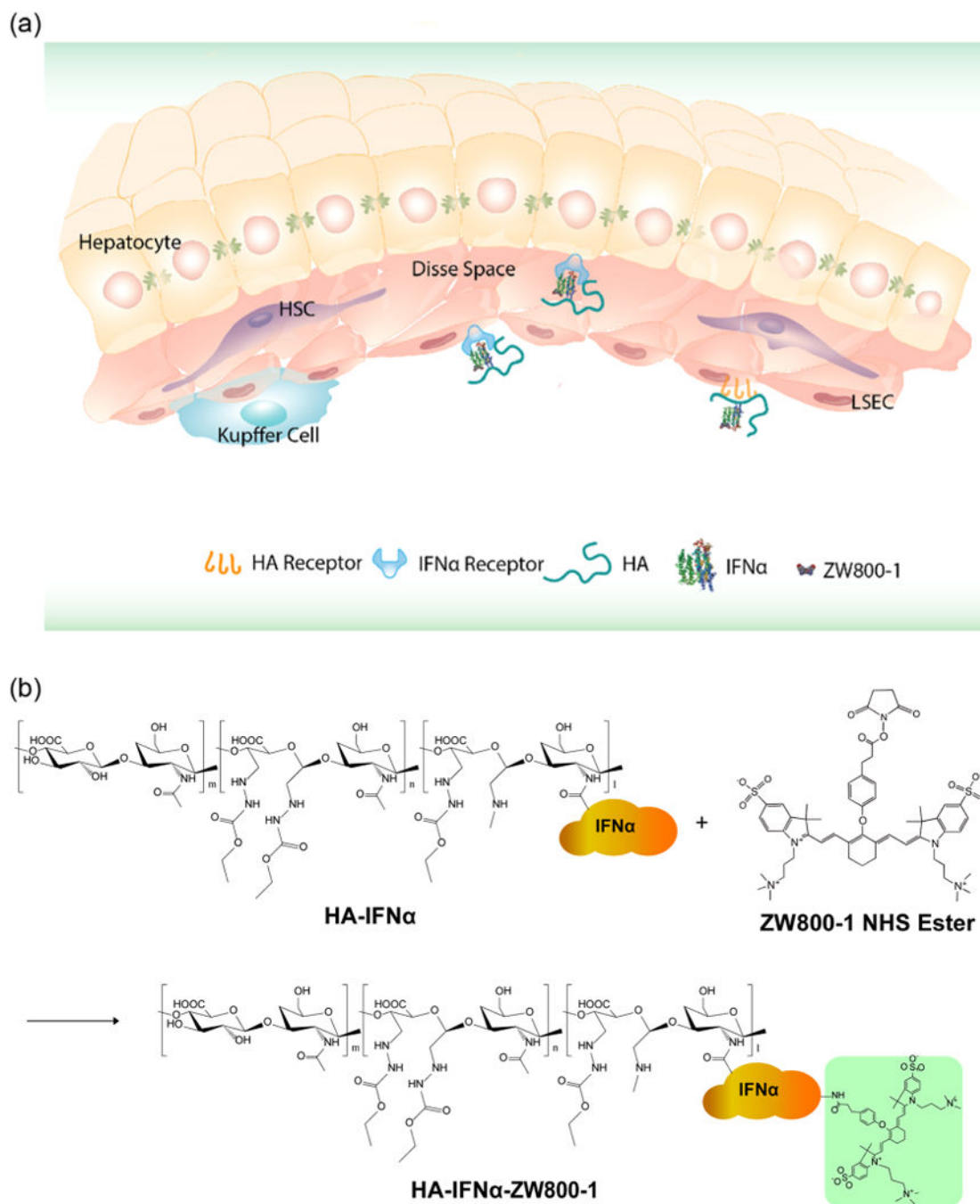**Figure 1.**
Schematic illustration of (a) the targeted delivery of HA–IFNα conjugates to the liver and (b) the labeling of the HA–IFNα conjugate with zwitterionic dye ZW800-1.
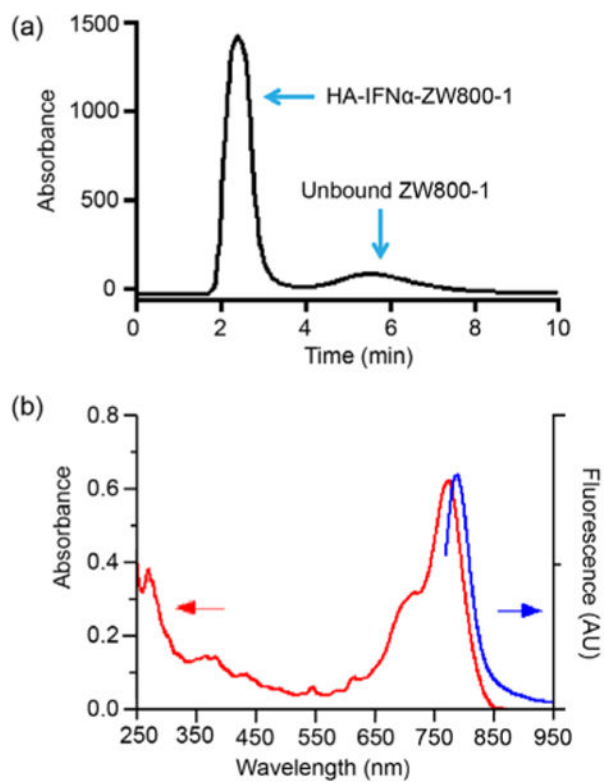
Figure 2.
Characterization of the HA–IFNα–ZW800-1 conjugate by (a) gel filtration chromatography and (b) spectrophotometry.
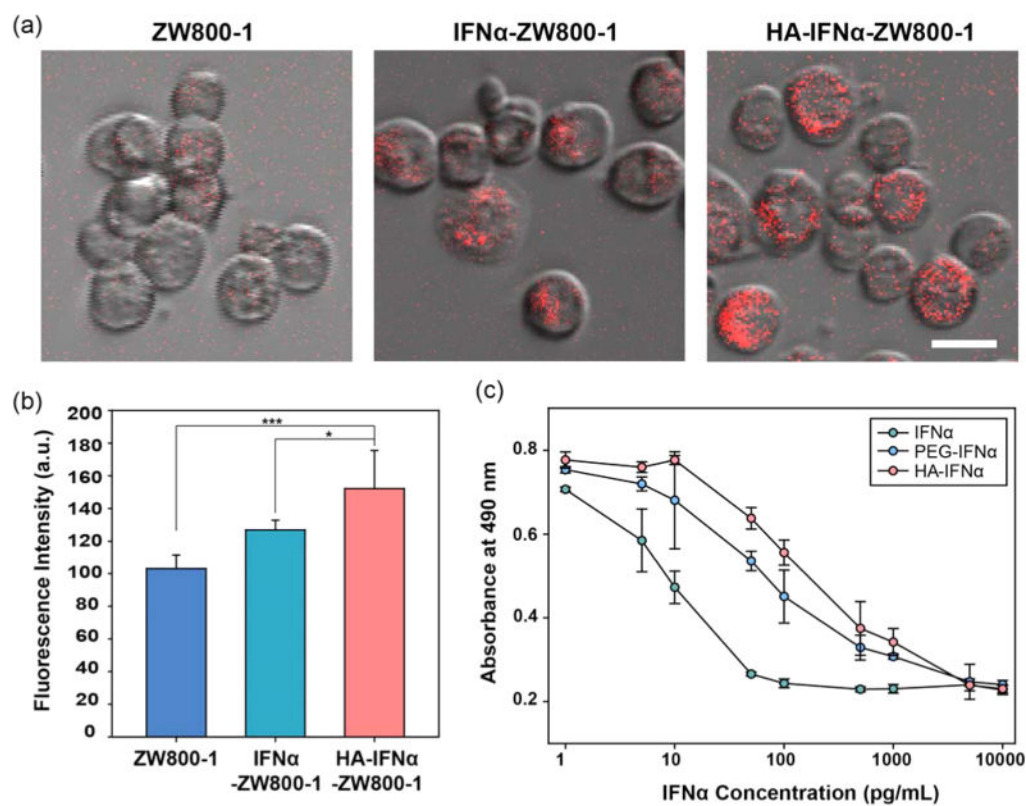
Figure 3.
(a) Confocal microscopic imaging of the intracellular uptake of ZW800-1, IFNa–ZW800-1, and HA–IFNa–ZW800-1 conjugates into HepG2 cells. (b) Quantitative fluorescence analysis of the samples taken up by HepG2 cells. Statistical analysis was conducted for the HA–IFN–ZW800-1 conjugate vs other groups (*$P < 0.05$, and ***$P < 0.001$). (c) Antiproliferation effect of IFNa, PEG–IFNa, and HA–IFNa conjugates in Daudi cells.
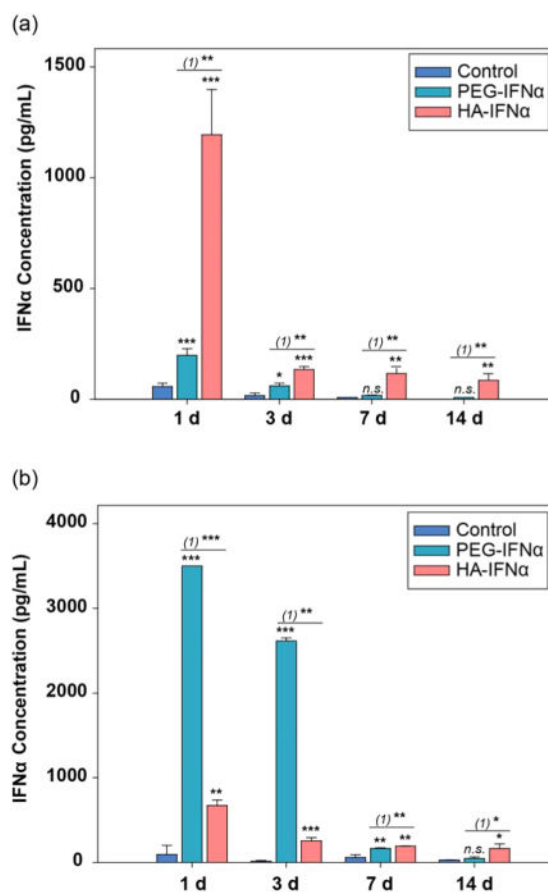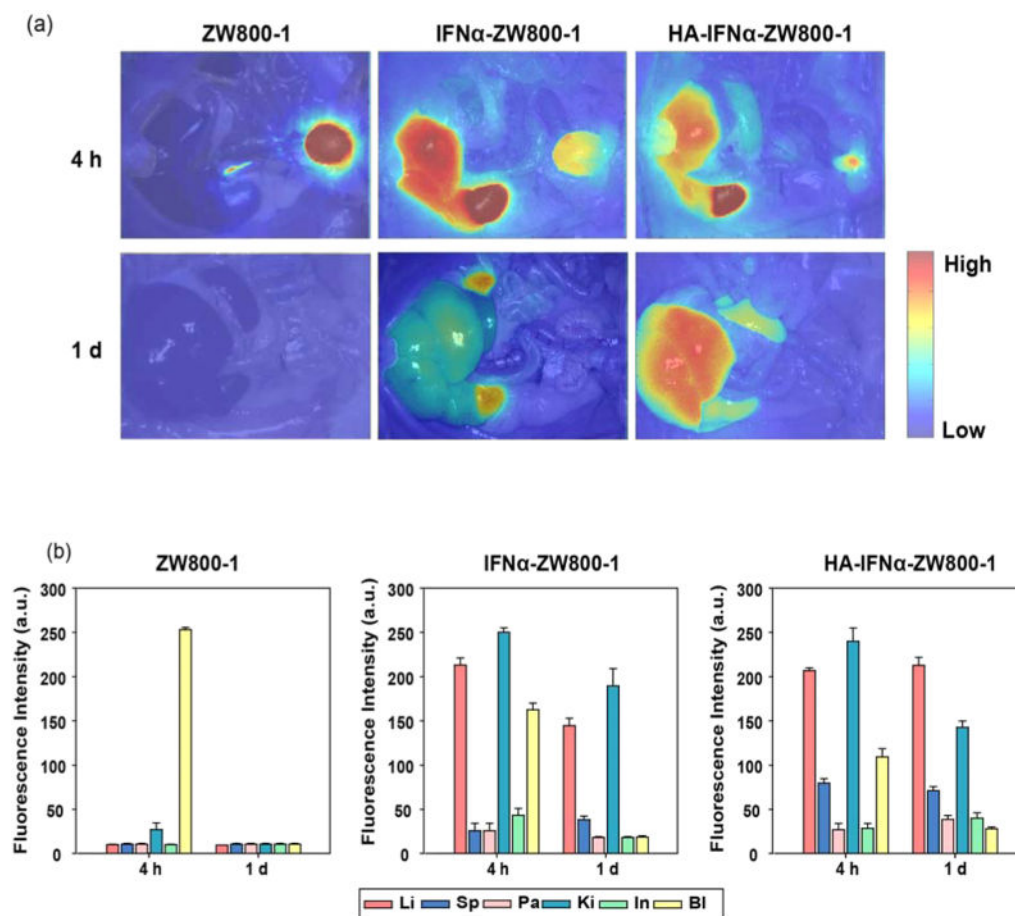
Figure 4.
Pharmacokinetic analysis of PEG–IFNα and HA–IFNα conjugates by an ELISA in (a) the liver and (b) blood serum after intravenous injection. PBS was used as a negative control. Statistical analysis was conducted for the control vs PEG–IFNα and HA–IFNα conjugates (*$P < 0.05$; **$P < 0.01$; ***$P < 0.001$). (1) represents the PEG–IFNα vs HA–IFNα conjugate.

Figure 5.
(a) *In vivo* biodistribution of ZW800-1, IFNa–ZW800-1, and HA–IFNa–ZW800-1 conjugate in SD rats 4 and 24 h after intravenous injection. (b) Quantitative fluorescence analysis of intraoperative major organs. Abbreviations: Li, liver; Sp, spleen; Pa, pancreas; Ki, kidney; In, intestine; Bl, bladder.
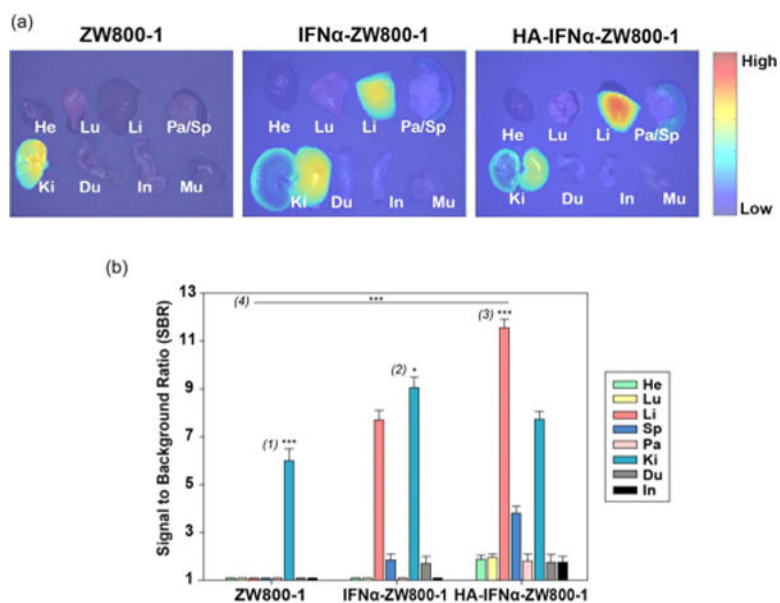
Figure 6.
(a) *Ex vivo* biodistribution of ZW800-1, IFNa–ZW800-1, and HA–IFNa–ZW800-1 conjugate in SD rats 24 h after intravenous injection. (b) Quantitative fluorescence analysis of dissected organs 24 h postinjection for the biodistribution. Abbreviations: He, heart; Lu, lung; Li, liver; Sp, spleen; Pa, pancreas; Ki, kidney; Du, duodenum; In, intestine. Statistical analysis was conducted for (1) kidney vs other organs treated with ZW800-1 (***$P < 0.001$), (2) kidney vs liver treated with IFNa-ZW800-1 (*$P < 0.05$), (3) liver vs other organs treated with the HA–IFNa–ZW800-1 conjugate (***$P < 0.001$), and (4) liver treated with the HA–IFNa–ZW800-1 conjugate vs IFNa–ZW800-1 and ZW800-1 (***$P < 0.001$).
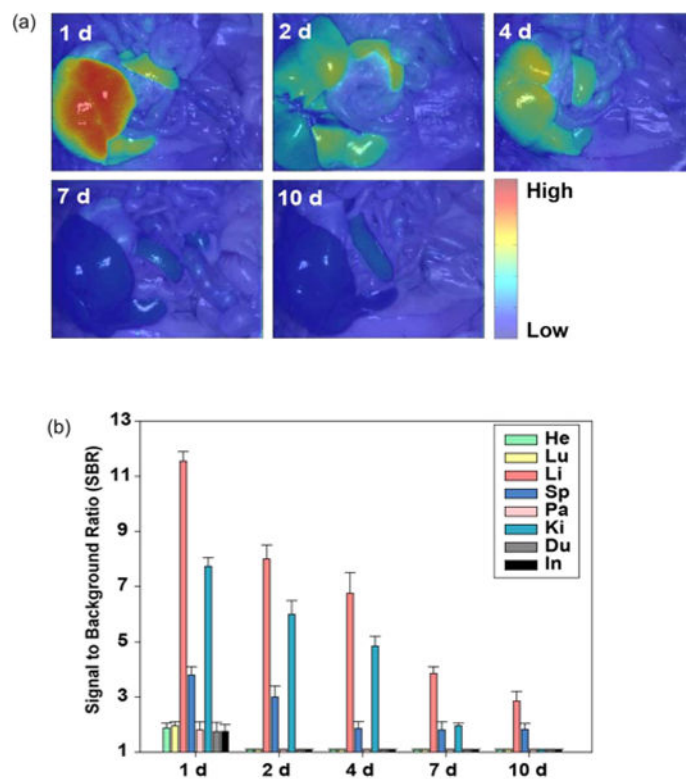
Figure 7.
(a) Intraoperative fluorescence images and (b) quantitative analysis for long-term biodistribution and clearance of HA–IFNa–ZW800-1 conjugates for up to 10 days after intravenous injection. Abbreviations: He, heart; Lu, lung; Li, liver; Sp, spleen; Pa, pancreas; Ki, kidney; Du, duodenum; In, intestine.
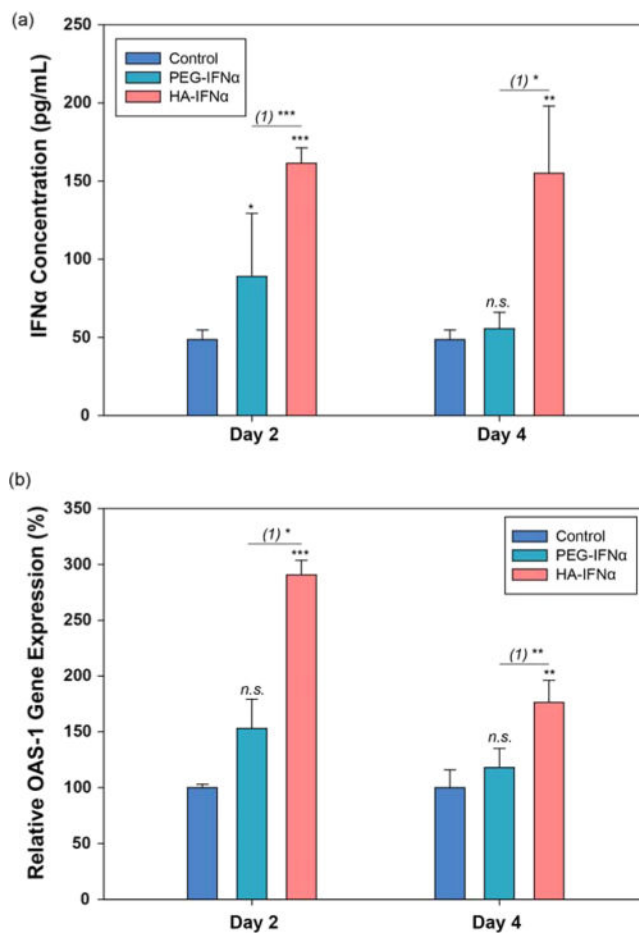
Figure 8.
(a) Pharmacokinetic analysis of PEG–IFNα and HA–IFNα conjugates by an ELISA in the liver after subcutaneous injection. PBS was used as a negative control. (b) Relative level of OAS1 mRNA in the liver by RT-PCR after subcutaneous injection of the control of PBS, PEG–IFNα, and HA–IFNα conjugate. Statistical analysis was conducted for the control vs PEG–IFNα and HA–IFNα conjugates (*$P < 0.05$; **$P < 0.01$; ***$P < 0.001$). (1) represents PEG–IFNα vs HA–IFNα conjugate.